Continuous-wave operation of 2.7 THz photonic crystal quantum cascade lasers

G. Sevin, D. Fowler, G. Xu, F.H. Julien, R. Colombelli, H. Beere and D. Ritchie

Continuous-wave laser action has been achieved in a 2.7 THz quantum cascade device operating on the modes of a two-dimensional photonic crystal resonator. The photonic structure is patterned into the device top metal contact layer. The emission is obtained from the device surface. It is single lobed and highly directional. At cryogenic temperatures the output power is ≃300 μW.

Introduction: Since their inception in 2002 [1], advances in long wavelength (60–300 μm) quantum cascade laser (QCL) designs have rapidly established this technology as the leading candidate for compact semiconductor sources of coherent terahertz radiation. While improvements in the design and performance of the QCL active region (AR) have slowed in recent years, leading to a stagnation of the maximum operation temperature T_{max} of 186 K [2], constant refinement of the applied waveguide technology is addressing other important aspects of the device performance, in particular, the quality of the output beam pattern.

Currently, the most efficient solution for a terahertz QCL waveguide relies on the tranverse magnetic (TM)-polarised plasmonic modes at the upper and lower interfaces between the dielectric semiconductor AR and metallic contact layers [3, 4], in so-called metal–metal waveguides. However, the consequent sub-wavelength vertical light confinement leads to highly divergent output beams from the laser facets [5]. Several strategies have been investigated to achieve more directional light output, in either edge or surface-emitting configurations, while maintaining low threshold current densities (J_{th}) and high T_{max} [6–8]. One such approach is the photonic crystal resonator in which single frequency surface emission can be achieved by patterning the upper metallic contact layer, at the expense of generally slightly higher waveguide losses and thus lower T_{max} compared with standard Fabry-Perot ridge resonators [9–11].

Continuous-wave (CW) laser operation is dependent on the dissipation of heat through the relatively high thermal resistance material of the QCL device, such that the effective temperature within the AR does not exceed T_{max}. Thus, CW laser action may be promoted not only by improving the heat flow within the device, but also by reducing the J_{th} of a laser, either by refining the AR energy band structure or by enhancing the overall Q factor of the resonator.

In this Letter, we implement a refined PhC design which allows CW singlemode laser operation at $\nu = 2.7$ THz up to a heatsink temperature of 39 K, whilst maintaining highly directional and monochromatic surface emission. The target application of these devices is local oscillators for heterodyne detection, typically for astronomic detection applications [12], where cryogenic operation and hundreds of μW of output power are acceptable performance constraints.

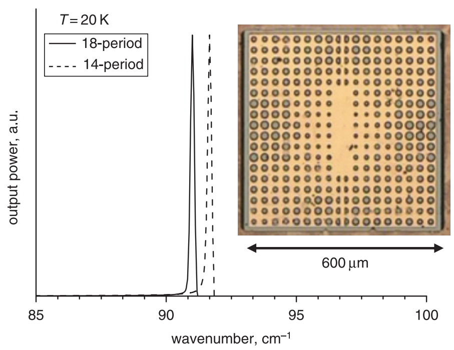

Fig. 1 *Typical emission spectra of lasers under CW operation. Measurements performed at $T = 20$ K, with Fourier transform infrared spectrometer (resolution: 0.125 cm^{-1}) and DTGS detector*

Inset: Surface view of 18-period photonic crystal device. Uniformly metallised central region used for application of bonding wire

Sample structure and design: The MBE-grown GaAs/AlGaAs 'bound to continuum' AR (described in [13]) is processed into 18-period (see Fig. 1, inset) and 14-period PhC devices [14]. The bare 15 μm-wide borders of the PhC rely on the 200 nm-thick, highly doped top contact layer to ensure absorbing boundary conditions which are crucial to the PhC mode operation [9]. The vertical confinement within the 12 μm-thick AR is provided by upper and lower gold metallic layers. The upper gold layer is patterned with a network of air holes to periodically modulate the light phase velocity in the device thus providing a laser resonator via the implementation of a 2D photonic crystal [9]. The grading of the hole size has been carefully optimised to enhance the in-plane factor ($Q_{//}$), increasing the waveguide efficiency for a lower J_{th}. The further introduction of a π phase-shift in the centre of the PhC structure leads to single lobed surface emission [14]. Finally, the upper contact bonding wire is connected in the centre of the device, avoiding the need for a separate bonding pad and maximising the device symmetry, whilst (counter intuitively) not affecting the device far field characteristics, as shown in [15].

Measurements, results and discussion: Typical spectra of the devices in CW operation mode are shown by the solid/dashed lines in Fig. 1. The emission is singlemode, at a frequency $\nu \simeq 2.7$ THz. The slight frequency shift between the two PhC sizes is owing to the small change in the frequency of the finite-size monopolar mode at the PhC Γ-point as a function of the resonator dimension.

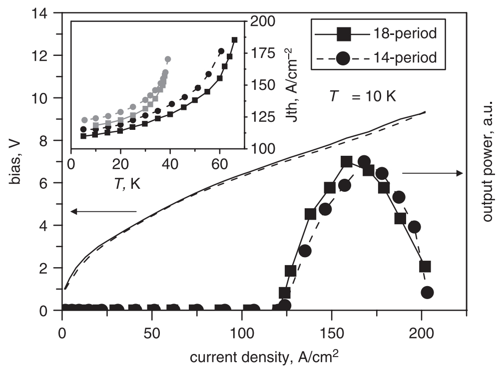

Fig. 2 *LIV characteristics for 18-period (continuous line, square symbols) and 14-period devices (dashed line, round symbols) measured at $T =$ 10 K and in continuous wave (CW)*

Inset: Laser threshold current density against heatsink temperature in both pulsed (black lines) and continuous wave operation (grey lines). Continuous lines, square symbols correspond to 18-period devices, while dashed lines, round symbols to 14-period devices

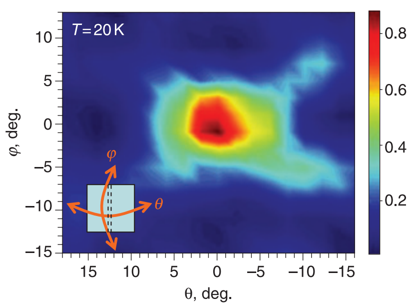

Fig. 3 *Far field surface-emission pattern of 18-period PhC THz laser. Measurement performed at $T = 20$ K by scanning Golay cell on sphere at constant distance (≃10 cm) from laser surface, in steps of 2°*

Fig. 2 shows the CW light-current-voltage (LIV) characteristics at a heatsink temperature $T = 10$ K for both devices. The J_{th} in CW is 120 (124) A/cm^2 for the 18-period (14-period) device, corresponding to absolute threshold currents (I_{th}) of 430 (285) mA. The small difference in J_{th} for the two devices is owing to changes in the $Q_{//}$ factor, which decreases with a reduction in PhC size [14, 15]. The inset of Fig. 2 shows $J_{th}(T)$, the J_{th} dependence on the heatsink temperature, for both devices in pulsed (4% duty-cycle) and CW operation. The J_{th} increases rapidly with temperature under CW operation, owing to the reduced dissipation of thermal energy which leads to temperatures in the AR significantly larger than those of the heatsink. The maximum operating heatsink temperature is 66 (60) K in pulsed and 38 (39) K in CW operation. The maximum output power in CW was estimated using a thermopile and it was found to be, for both devices, in the 200 to 400 μW range.

Fig. 3 presents the characterisation of the surface-emission patterns in the far field for an 18-period PhC device at T = 20 K with $I = 600$ mA. It were acquired by scanning a Golay cell on a sphere at constant radius from the laser surface. The beam pattern exhibits an almost ideal, single-lobed and angularly-narrow emission shape, with an approximate full-width half-maximum (FWHM) of $10 \times 10^{\circ}$ and a directivity (as defined in [16]) $D \simeq 19-20$ dB.

Conclusion: By using a terahertz QCL based on a bound-to-continuum design, which has a significantly reduced J_{th} ($\simeq$100 A/cm^2 compared to $\simeq$850 A/cm^2 in [14]), we have demonstrated CW operation (at cryogenic temperatures) of a surface-emitting, photonic crystal laser at $\nu \simeq$ 2.7 THz. The optimised PhC device architecture yields a lower J_{th} and a higher T_{max} than a standard, non-optimised PhC design would [14], as well as a highly directional, single lobed emission pattern [15].

Acknowledgments: The device fabrication has been performed at the nanocentre CTU-IEF-Minerve, partially funded by the 'Conseil Général de l'Essonne'. This work was conducted as part of a EURYI scheme award (see www.esf.org/euryi). It was also supported by the French National Research Agency (ANR-09-NANO-017 'Hi-Teq').

23 July 2010

doi: 10.1049/el.2010.2036

One or more of the Figures in this Letter are available in colour online.

G. Sevin, D. Fowler, G. Xu, F.H. Julien and R. Colombelli (*Institut d'Electronique Fondamentale, Univ. Paris Sud, UMR8622 CNRS, 91405 Orsay, France*)

E-mail: raffaele.colombelli@u-psud.fr

H. Beere and D. Ritchie (*Cavendish Laboratory, University of Cambridge, Cambridge, United Kingdom*)

References

1 Köhler, R., Tredicucci, A., Beltram, F., Beere, H.E., Linfield, E.H., Davies, A.G., Ritchie, D.A., Iotti, R.C., and Rossi, F.: 'Terahertz semiconductor-heterostructure laser', *Nature* (UK), 2002, **417**, pp. 156–159

2 Kumar, S., Hu, Q., and Reno, J.L.: '186 K operation of terahertz quantum-cascade lasers based on a diagonal design', *Appl. Phys. Lett.*, 2009, **94**, article ID 131105

3 Unterrainer, K., Colombelli, R., Gmachl, C., Capasso, F., Hwang, H.Y., Sergent, A.M., Sivco, D.L., and Cho, A.Y.: 'Quantum cascade lasers with double metal-semiconductor waveguide resonators', *Appl. Phys. Lett.*, 2002, **80**, article ID 3060

4 Kohen, S., Williams, B., and Hu, Q.: 'Electromagnetic modelling of terahertz quantum cascade laser waveguides and resonators', *J. Appl. Phys.*, 2005, **97**, article ID 053106

5 Gellie, P., Maineult, W., Andronico, A., Leo, G., Sirtori, C., Barbieri, S., Chassagneux, Y., Coudevylle, J.R., Colombelli, R., Khanna, S.P., Linfield, E.H., and Davies, A.G.: 'Effect of transverse mode structure on the far field pattern of metal-metal terahertz quantum cascade lasers', *J. Appl. Phys.*, 2008, **104**, article ID 124513

6 Maineult, W., Gellie, P., Andronico, A., Filloux, P., Leo, G., Sirtori, C., Barbieri, S., Peytavit, E., Akalin, T., Lampin, J.-F., Beere, H.E., and Ritchie, D.A.: 'Metal-metal terahertz quantum cascade laser with mid-transverse-electromagnetic-horn antenna', *Appl. Phys. Lett.*, 2008, **93**, article ID 183508

7 Amanti, M.I., Fischer, M., Scalari, G., Beck, M., and Faist, J.: 'Low-divergence single-mode terahertz quantum cascade laser', *Nat. Photonics*, 2009, **3**, (10), pp. 586–590

8 Kumar, S., Williams, B.S., Qin, Q., Lee, A.W.M., and Hu, Q.: 'Surface-emitting distributed feedback terahertz quantum-cascade lasers in metal-metal waveguides', *Opt. Express*, 2007, **15**, pp. 113–128

9 Chassagneux, Y., Colombelli, R., Maineult, W., Barbieri, S., Beere, H.E., Ritchie, D.A., Khanna, S.P., Linfield, E.H., and Davies, A.G.: 'Electronically pumped photonic-crystal terahertz lasers controlled by boundary conditions', *Nature*, 2009, **457**, pp. 174–178

10 Chassagneux, Y., Colombelli, R., Maineult, W., Barbieri, S., Khanna, S.P., Linfield, E.H., and Davies, A.G.: 'Predictable surface emission patterns in terahertz photonic-crystal quantum cascade lasers', *Opt. Express*, 2009, **17**, pp. 9491–9502

11 Xu, G., Chassagneux, Y., Colombelli, R., Beaudoin, G., and Sagnes, I.: 'Polarised signle-lobed surface emission in mid-infrared, photonic crystal, quantum cascade lasers', *Opt. Lett.*, 2010, **35**, pp. 859–861

12 Siegel, P.H.: 'Terahertz technology', *IEEE Trans. Microw. Theory Tech.*, 2002, **50**, pp. 910–928

13 Chassagneux, Y., Palomo, J., Colombelli, R., Barbieri, S., Dhillon, S., Sirtori, C., Beere, H., Alton, J., and Ritchie, D.: 'Low threshold THz QC lasers with thin core regions', *Electron. Lett.*, 2007, **43**, pp. 285–286

14 Chassagneux, Y., Colombelli, R., Maineult, W., Barbieri, S., Khanna, S.P., Linfield, E.H., and Davies, A.G.: 'Graded photonic crystal terahertz quantum cascade lasers', *Appl. Phys. Lett.*, 2010, **96**, article ID 031104

15 Sevin, G., Fowler, D., Xu, G., Julien, F.H., Colombelli, R., Khanna, S.P., Linfield, E.H., and Davies, A.G.: 'Optimised surface-enithing photonic-crystal terahertz quantum cascade lasers with reduced resonator dimensions', *Appl. Phys. Lett.*, 2010, **97**, article ID 131101

16 Yu, N., Blanchard, R., Fan, J., Wang, Q., Pflügl, C., Diehl, L., Edamura, T., Yamanishi, M., Kan, H., and Capasso, F.: 'Quantum cascade lasers with integrated plasmonic antenna-array colliniators', *Opt. Express*, 2008, **16**, pp. 19447–19461